

Quantized Faraday effect in (3+1)-dimensional and (2+1)-dimensional systems

L. Cruz Rodríguez,^{1,*} A. Pérez Martínez,^{2,†} H. Pérez Rojas,^{2,‡} and E. Rodríguez Querts^{2,§}

¹*Departamento de Física General, Facultad de Física,
Universidad de la Habana, San Lázaro y L, Vedado La Habana, 10400, Cuba*

²*Instituto de Cibernética Matemática y Física (ICIMAF)
Calle E esq 15 No. 309 Vedado, La Habana, 10400, Cuba*

We study Faraday rotation in the quantum relativistic limit. Starting from the photon self-energy in the presence of a constant magnetic field the rotation of the polarization vector of a plane electromagnetic wave which travel along the fermion-antifermion gas is studied. The connection between Faraday Effect and Quantum Hall Effect (QHE) is discussed. The Faraday Effect is also investigated for a massless relativistic (2D+1)-dimensional fermion system which is derived by using the compactification along the dimension parallel to the magnetic field. The Faraday angle shows a quantized behavior as Hall conductivity in two and three dimensions.

I. INTRODUCTION

Plane-polarized light penetrating in a magnetized transparent charged medium and moving parallel to the magnetic field \mathbf{B} rotates its plane of polarization as a consequence of birefringence: the incoming wave splits in two opposite circularly polarized modes moving with different speeds (and frequencies), and the polarization vector rotates. This is the Faraday effect [1].

Faraday rotation (FR) is clearly manifest for photon propagation parallel to the magnetic field. The symmetry properties behind the Faraday effect are the following: the field \mathbf{B} (which we take along the x_3 axis), breaks the Lorentz symmetry group in two subgroups, the translations along x_3 (leading to the conservation of momentum component p_3), and the rotations around x_3 (leading to the conservation of angular momentum J_3). The generator of rotations around J_3 is the antisymmetric matrix $A_{3ij} = -A_{3ji} = \delta_{i1}\delta_{j2}$ whose eigenvectors are proportional to the complex unit vectors $\mathbf{e}^\pm = (\mathbf{e}_1 \mp i\mathbf{e}_2)/\sqrt{2}$, where \mathbf{e}^\pm are related respectively to positive and negative circular polarizations. If the system is C invariant, both opposite circular polarizations contribute symmetrically, leading to equal speeds of light propagating along \mathbf{B} . If the system is noninvariant under C , the speeds of light differ for opposite circular polarizations. The resulting polarization vector rotates describing a circumference (in general an ellipse), and the Faraday effect arises.

For propagation perpendicular to \mathbf{B} , two elliptically polarized modes arise, one of their semiaxes being along the propagation vector k , the rotation being in the plane orthogonal to \mathbf{B} containing \mathbf{k} [2]-[4].

The FR is indeed a particular case of the general problem of photon propagation in a charged medium [5]. In nonrelativistic media, like the ionosphere and insulators it is a well-known phenomena where the classical and semiclassical approaches can be applied successfully [1].

However, FR effects have been also observed in electromagnetic waves coming from astrophysical objects [6]. Some of these sources are compact objects which are characterized by high densities and strong magnetic fields that can reach up to 10^{15} G in magnetars [7]. Hence the physical process involved in the case of compact objects requires an adequate treatment from the point of view of a quantum-relativistic approach.

On the other hand, in quasiplanar condensed matter systems such as graphene (a genuine monolayer of carbon atoms in a honeycomb array, whose theoretical properties are essentially described by a two-dimensional relativistic chiral fermion system [8]-[10]), FR is observed when light propagates perpendicular to the graphene layer in the presence of a static magnetic field with $\mathbf{k} \parallel \mathbf{B}$ and the relation between the Faraday angle and the nonstatic ($\omega \neq 0$) Hall conductivity has been pointed out [11]-[14].

From the point of view of novel applications of graphene, magneto-optical phenomena such as Faraday effect must be understood from both the theoretical and experimental points of view. Theoretical studies of the conductivity tensor in the static limit [10], [15] and nonstatic regime have been done [16]-[17]. Recently, FR has been detected in single-layer and multilayered epitaxial graphene [18]. The measure-

* lcruz@fisica.uh.cu

† aurora@icimaf.cu

‡ hugo@icimaf.cu

§ elizabeth@icimaf.cu

ments report a giant value of the rotation angle which comes exclusively from the graphene system (the substrate did not show any FR).

In spite of the differences in contexts, the description of the Faraday effect in both, the astrophysical and graphene scenarios, can be theoretically tackled by considering photon propagation parallel to the constant magnetic field in quantum-relativistic dense matter.

The scope of the present paper is to describe the FR effect and to obtain the Faraday angle for (3+1)-dimensional (3D+1) and 2+1 dimensional (2D+1) systems, starting from the same formalism: the relativistic conductivity tensor in 3D+1 for a massive fermion system. Our goal will be to show the connection between Hall conductivity and the Faraday effect and the quantization of the Faraday angle [19].

In a previous paper [10], the Hall conductivity for a massless relativistic fermion system was studied by starting from the quantum-relativistic photon self-energy tensor in the QED framework using the approach of Ref. [20] to obtain the static limit. Now, as we are interested in FR, this problem should be generalized to the nonstatic limit ($\omega \neq 0$).

In Ref. [5] a detailed study of the structure of the photon self-energy in the presence of a magnetic field at finite density and temperature was done. Photon self-energy satisfies properties of gauge and Lorentz and *CPT* invariance. General properties of the photon self-energy and the dispersion equations for photons propagating in the medium were solved in two cases: photon propagating parallel and perpendicular to the magnetic field [5].

In this paper we focus on the propagation parallel to the magnetic field which establishes a relation between the Hall and Faraday effects, so we take advantage of these calculations. We have also particularized the study to 2D+1 with the aim to describe graphene-like systems.

Our calculations have been done in the imaginary-time formalism. For $3D + 1$ and $2D + 1$ systems we have obtained the FR angle that the light undergoes upon propagating in a dense fermion system where the chemical potential μ is greater than temperature T ($\mu \gg T$).

The weak-field limit for light propagating in a magnetized plasma was studied in [21], taking the dependence of the self-energy with regard to \mathbf{B} in a linear approximation. In Ref. [22] a calculation of the photon self-energy is made for strong and moderate fields but $\mu \gg eB$. In both papers the Faraday effect is considered in some particular cases and the semiclassical results have been reproduced. The real-time formalism was used in Refs. [21]-[22].

ism was used in Refs. [21]-[22].

Our findings are relevant for two main reasons: first, we have extended them to the nonstatic limit from previous calculation [20]-[10] of 3D+1 relativistic massive fermions and 2D+1 relativistic massless Hall and Ohm conductivities. Second, we have found the connection between FR angle and Hall conductivity (the Faraday angle depends on the admittivity: complex conductivity, but the leading term is proportional to the Hall conductivity). This result for 3D+1 and 2D+1 systems shows that it is a consequence of general properties of QED in external magnetic fields at finite density. The angle as a function of the photon frequency ω has branching points for 3D+1 relativistic dense massive fermion systems as well as for 2D+1 massless systems a discrete set of ω values. Hence, FR shows the effect of quantization of the quantum Hall effect at nonzero frequency. Our results for 2D+1 massless system are in agreement with previous theoretical work for FR in graphene reported in Refs. [12]-[14]. The 2D+1 results have been obtained from 3D+1 results by dimensional compactification.

Astrophysical applications of our findings on FR angle can be expected in the context of radiation propagating through neutron stars magnetospheres. This problem will be discussed in a forthcoming presentation.

The paper is organized as follows: In Sec. II we start from the one-loop approximation of the photon self-energy in the presence of a constant and uniform magnetic field and obtain the relativistic Hall and Ohm conductivities in the nonstatic approximation by generalizing the results obtained in Ref. [20]. In Sec. III the 3D+1 Faraday effect is discussed and the Faraday angle is obtained to first order as half of the Hall conductivity. Then, the 2D+1 massless QED limit is obtained, and the expression for the Hall and Ohm conductivities are written in Sec. IV. In Sec. V the Faraday effect and angle are discussed in 2D+1 dimensions obtaining the same dependence with regard to the Hall conductivity as the 3D+1 case in the first-order approximation. Finally, in Sec. VI we state the concluding remarks. Appendices show the calculations relevant to our results.

II. PHOTON SELF-ENERGY IN PRESENCE OF MAGNETIC FIELD

The photon self-energy in quantum electrodynamics in an external magnetic field was calculated at finite temperature and nonzero density in Ref. [2]. The total electromagnetic field is written $A_\mu^e + a_\mu$ where

A_μ^e refers to the external magnetic field and a_μ to the radiation field. The photon self-energy (also called the polarization operator), can also be interpreted as the linear-term coefficient of the functional expansion of the four-current j_μ in powers of the electromagnetic field a_μ . That is, $j_\mu = \Pi_{\mu\nu} a_\nu$.

The introduction of a chemical potential $\mu \neq 0$ is associated with a non-neutral electron-positron charged medium. The system is thus assumed as C noninvariant, and total charge neutrality is guaranteed by the assumption of a hadron background. This background, however, is not taken into account in any of the further calculations.

The generalized Furry's theorem [23] establishes that odd powers of μ will be associated with odd powers of A_μ^e through antisymmetric tensor structures. That is, the self-energy contains antisymmetric odd-in- μ terms. Also, as gauge invariance is satisfied, it implies that the self-energy tensor satisfies the four-dimensional gauge invariance condition $\Pi_{\mu\nu} k_\nu = k_\mu \Pi_{\mu\nu} = 0$. We have for the photon self-energy the expression¹

$$\Pi_{\mu\nu}(x, y) = e^2 \text{Tr} \int \gamma_\mu G(x, z) \Gamma_\nu(z, y', y) G(y', x) d^4 z d^4 y'. \quad (1)$$

For the calculation of the components of $\Pi_{\mu\nu}$ we take (1) in the one loop approximation with the temperature Green's functions $G(x, y|A^e)$ being the solution of the Dirac equation in a constant magnetic field \mathbf{B} such that $A_\nu^e = Bx_1 \delta_{\nu,2}$, directed along the x_3 -axis

$$[\gamma_\nu(\partial_\nu - ieA_\nu^e) + m]G(x, y|A^e) = \delta(x - y), \quad (2)$$

where $\partial_4 = \partial/\partial x_4 - \mu$, and μ is the chemical potential for the electron-positron gas. It is also important to remark that Eq. (2) defines the fermion temperature-dependent Green's function for x_4 in the interval $-\beta$ to β ; $\beta = 1/T$. In the one-loop approximation the Fourier transform of the polarization tensor has the form

$$\Pi_{\nu\rho}(k_4, \vec{x}, \vec{x}'|A^e) = \frac{e^2}{\beta} \text{Tr} \sum_{p_4} \gamma_\nu G(p_4, \vec{x}, \vec{x}'|A^e) \gamma_\rho G(p_4 + k_4, \vec{x}, \vec{x}'|A^e), \quad (3)$$

where $p_4 = (2s+1)\pi/\beta$ and s runs over integers from $-\infty$ to $+\infty$. Substituting the expression of the Green function of fermions $G(p_4, \vec{x}, \vec{x}'|A^e)$ we obtain the self-

energy tensor as

$$\Pi_{\nu\rho}(k|A^e, \mu, \beta^{-1}) = \frac{e^3 B}{2\pi^2 \beta} \sum_{p_4} \sum_{n, n'} \int \frac{dp_3 C_{\nu, \rho}}{[p_4^* + \epsilon_{p, n}^2][(p_4^* + k_4) + \epsilon_{p'}^2]}, \quad (4)$$

where $p_4^* = p_4 + i\mu$, $\epsilon_{p, n} = \sqrt{p_3^2 + m^2 + 2enB}$, $\epsilon_{p, n'} = \sqrt{(p_3 + k_3)^2 + m^2 + 2en'B}$, n and n' are the Landau numbers and in what follows we will use the notation $k_\perp^2 \equiv k_1^2 + k_2^2$ and $k_\parallel^2 = k_3^2 + k_4^2$. Let us remark that the presence of the magnetic field in the x_3 direction breaks the spatial symmetry, hence in Eq. (4) only the integral over dp_3 has survived. The integral over $\int dp_\perp \rightarrow \sum_n \frac{\alpha_n eB}{(2\pi)^2}$ where $\alpha_n = 2 - \delta_{n0}$.

As mention earlier, in Ref. [5] the structure of self-energy of the photon (4) in presence of a magnetic field at finite density and temperature was obtained by considering the properties of gauge and Lorentz invariance and CPT invariance. Six independent transverse tensors can be built in terms of the four vectors: the momentum of the photon k_μ , the product of the external electromagnetic field tensor $F_{\mu\rho}$ and its square by k_μ , leading respectively as $F_{\mu\rho} k_\rho$ and $F_{\mu, \rho}^2 k_\rho$, and the four-velocity of the medium u_μ (a summary of these properties can be found in the appendix). As our goal is to study the Faraday effect in connection to the conductivity tensor we will concentrate on the case of a photon propagating parallel to the magnetic field ($k_\perp = 0$) [5]; in that case only three scalars are independent. As we will show in the next sections only two of them are related to the conductivity and also to Faraday effect.

Relativistic Hall and Ohm conductivity in non-static limit ($\omega \neq 0$)

This section is devoted to studying the 3D+1 relativistic Hall and Ohm conductivities in the nonstatic limit ($\omega \neq 0$). The expression for the spatial part of the current density is linear in terms of the perturbative magnetic field and is given in terms of the photon self-energy of the medium by [20]

$$j_i = \Pi_{i\nu} a_\nu, \quad i = 1, 2, 3, \quad \nu = 1, 2, 3, 4 \quad (5)$$

where $a_4 = ia_0$ and $k_4 = i\omega$, having in mind the transversality condition given by $\Pi_{\mu\nu}(k)k_\nu = 0$, due to gauge invariance, Eq. (5) can be written as

$$j_i = Y_{ij} E_j, \quad i = 1, 2, 3, \quad j = 1, 2, 3 \quad (6)$$

where $Y_{ij} = \Pi_{ij}/i\omega$ is the admittivity (complex conductivity tensor) and $E_j = i(\omega a_j - k_j a_0)$ is the electric field.

¹ Unless specified otherwise, we use natural units $\hbar = c$.

We will be especially interested in the real conductivity $\sigma_{ij} = \text{Re}[Y_{ij}]$. The contribution to the current density in Eq. (6) due to σ_{ij} can be written as

$$j_i = \sigma_{ij}^0 E_j + (E \times S)_i, \quad (7)$$

where $\sigma_{ij}^0 = \frac{\text{Im}[\Pi_{ij}^S]}{\omega}$ and $S_i = \frac{1}{2}\epsilon^{ijk}\sigma_{jk}^H$ is a pseudovector associated with $\sigma_{ij}^H = \frac{\text{Im}[\Pi_{ij}^A]}{\omega}$. Π_{ij}^A and Π_{ij}^S are, respectively, the antisymmetric and symmetric parts of the polarization tensor [10] and [20].

In the particular case where the electric field is the polarization vector of a transverse wave propagating along the magnetic field \mathbf{B} , being $\mathbf{E} \perp \mathbf{B}$, the conductivity tensor can be written in the following way:

$$\sigma_{ij} = \sigma^0 \delta_{ij} + \epsilon_{ij} \sigma^H, \quad (8)$$

where ϵ_{ij} is the antisymmetric 2×2 unity tensor, $\epsilon_{12} = -\epsilon_{21} = 1$ and

$$\sigma^0 = \text{Im}[t]/\omega, \quad (9)$$

$$\sigma^H = \text{Im}[r]/\omega, \quad (10)$$

where the scalar quantities r and t depend on the frequency- ω , the momentum k_3 and also the temperature, chemical potential and magnetic field [5]. From Eq. (8) we can identify σ^0 , σ^H with the Ohm and Hall conductivities respectively. The scalar r can be written as

$$r(k_{\parallel}, \mu, B, T) = iI_r, \quad (11)$$

and I_r is the integral

$$I_r = \frac{e^3 B \omega}{2\pi^2} \sqrt{\frac{k_{\parallel}^2}{k_{\parallel}^2}} \sum_{n,n'} F_{n,n'}^{(3)}(0) \int_{-\infty}^{\infty} \frac{dp_3 (k_{\parallel}^2 + 2eB(n+n'))}{D} \times (n_e(\varepsilon_{p,n}) - n_p(\varepsilon_{p,n})), \quad (12)$$

$$D = [2p_3 k_3 + k_{\parallel}^2 + 2eB(n' - n)]^2 - 4\omega^2 \varepsilon_{p,n}^2. \quad (13)$$

for $k_{\perp} \sim 0$, $\sqrt{\frac{k_{\parallel}^2}{k_{\parallel}^2}} \rightarrow 1$, $n_{e,p}(\varepsilon_{p,n}) = (1 + e^{(\varepsilon_{p,n} \mp \mu)\beta})^{-1}$ are the Fermi-Dirac distribution for fermions and antifermions, respectively. The scalar t is

$$t(k_{\parallel}, \mu, B, T) = -\frac{e^3 B}{4\pi^2} \sum_{n,n'} F_{n,n'}^{(2)}(0) I_t, \quad (14)$$

where $F_{n,n'}^{(2,3)}(0) = \delta_{n,n'-1} \pm \delta_{n-1,n'}$ and I_t

$$I_t = \int_{-\infty}^{\infty} \frac{dp_3}{\varepsilon_{n,p}} \left(1 - \frac{(2p_3 k_3 + J_{nn'})(k_{\parallel}^2 + 2eB(n+n'))}{D}\right) \times (n_e(\varepsilon_{p,n}) + n_p(\varepsilon_{p,n})) \quad (15)$$

and $J_{nn'} = k_{\parallel}^2 + 2eB(n' - n)$.

Thus, we have the expressions for the scalars r and t in the one loop approximation for the fermion-antifermion gas, with the assumption of $k_{\perp} = 0$. Now, starting from them we can study the Hall and Ohm conductivities in some particular limits which are relevant for applications in astrophysics as well as in graphene-like systems.

A. 3D+1 Hall conductivity $\omega \neq 0$

The Hall and Ohm conductivities Eqs. (9) and (10) are given as imaginary parts of the scalars r and t respectively. At frequencies different from zero the integrals (12) and (15) have singularities which come from the zeros of the denominator D . But the Hall conductivity is the imaginary part of $r = iI_r$, thus the contribution to the Hall conductivity comes from the real part of I_r , which means to consider the principal value of the integral [see the appendix, first term of (A39)]. The result is the following:

$$\text{Im}[r(k_{\parallel}, B, \mu, T)] = \text{Re}[I_r], \quad (16)$$

where

$$\text{Re}[I_r] = P \left(\frac{e^3 B \omega}{2\pi^2} \sum_{n,n'} F_{n,n'}^{(3)}(0) \int_{-\infty}^{\infty} dp_3 \frac{(k_{\parallel}^2 + 2eB(n+n'))}{D} \times (n_e(\varepsilon_{p,n}) - n_p(\varepsilon_{p,n})) \right). \quad (17)$$

The denominator in (17) can be written as $D = 4k_{\parallel}^2(p_3 - p_3^{(1)})(p_3 - p_3^{(2)})$, where $p_3^{(1,2)}$ are the roots of the equation $D = 0$ (see details in [5])

$$p_3^{(1,2)} = \frac{-k_3 J_{nn'} \pm \omega \Lambda}{2k_{\parallel}^2}, \quad (18)$$

and

$$\Lambda = (J_{nn'}^2 + 4\varepsilon_{0,n}^2 k_{\parallel}^2)^{1/2}, \quad (19)$$

and we have for σ_H^{3D}

$$\sigma_H^{3D}(k_{\parallel}, B, \mu, T) = \frac{\text{Im}[r]}{\omega} = \frac{\text{Re}[I_r(k_{\parallel}, B, \mu, T)]}{\omega}, \quad (20)$$

In the degenerate limit where $\mu \gg T$ and $n_e(\epsilon_{p,n})$ are replaced by a step functions $\theta(\mu - \epsilon_{p,n})$, $n_p(\epsilon_{p,n}) \rightarrow 0$, after integration we obtain

$$\sigma_H^{3D}(k_{\parallel}, B, \mu, T) = -\frac{e^3 B}{2\pi^2} \sum_{n,n'}^{n_{\mu}, n'_{\mu}} F_{n,n'}^{(3)}(0) \frac{k_{\parallel}^2 + 2eB(n+n')}{4\omega\Lambda} (\ln |\frac{p_f - p_3^{(2)}}{p_f + p_3^{(2)}}| + \ln |\frac{p_f + p_3^{(1)}}{p_f - p_3^{(1)}}|), \quad (21)$$

where $p_f = \sqrt{\mu^2 - m^2 - 2neB}$ is the Fermi momentum. As $F_{n,n'}^{(3)}(0)$ are given by Kronecker δ expressions and taking the long wave limit $k_3 \rightarrow 0$ we have for σ_H^{3D} the expression

$$\begin{aligned} \sigma_H^{3D}(\omega, B, \mu, 0) = & \frac{e^3 B}{2\pi^2} \left(\sum_{n=0}^{n_{\mu}} \frac{\omega^2 - 2eB(2n+1)}{4m_n\omega^2} \frac{1}{\sqrt{(\frac{2eB-\omega^2}{2\omega m_n})^2 - 1}} \ln \left| \frac{p_f/m_n - \sqrt{(\frac{2eB-\omega^2}{2\omega m_n})^2 - 1}}{p_f/m_n + \sqrt{(\frac{2eB-\omega^2}{2\omega m_n})^2 - 1}} \right| \right. \\ & \left. - \sum_{n=1}^{n_{\mu}} \frac{\omega^2 - 2eB(2n-1)}{4m_n\omega^2} \frac{1}{\sqrt{(\frac{2eB+\omega^2}{2\omega m_n})^2 - 1}} \ln \left| \frac{p_f/m_n - \sqrt{(\frac{2eB+\omega^2}{2\omega m_n})^2 - 1}}{p_f/m_n + \sqrt{(\frac{2eB+\omega^2}{2\omega m_n})^2 - 1}} \right| \right). \end{aligned} \quad (22)$$

where $m_n = \sqrt{m^2 + 2neB}$. From Eq. (17) at zero frequency $\omega = 0$ (static limit) we recover the quantum Hall conductivity obtained in Ref. [20]:²

$$\sigma_H^{3D}(0, B, \mu, T) = \frac{e^2}{h^2} \sum_n^{n_{\mu}} \alpha_n \int_{-\infty}^{\infty} dp_3 \theta(\mu - \epsilon_{p,n}) = \frac{e^2}{ch^2} \sum_n^{n_{\mu}} \alpha_n p_f. \quad (23)$$

The sum over Landau levels is up to the integer number $n_{\mu} = I[(\mu^2 - m^2)/(2eB)]$, $n'_{\mu} = n_{\mu} + 1$.

In Fig. 1, the three-dimensional (3D) nonstatic Hall conductivity is plotted for constant chemical potential and frequency as a function of the magnetic field. The curved step behavior is illustrated; this behavior is also observed in the static limit [20].

B. 3D+1 Ohm conductivity $\omega \neq 0$

Our aim now is to calculate the Ohm conductivity given by Eq. (9). A detailed calculation of $\text{Im}[t]$ can be found in [5]. Its expression comes from the imaginary part of the integral (15), which is related to the singularities due to absorptive process, and it can be written in two different cases, the first one, where $k_{\parallel}^2 > 0$, and absorption is only due to excitation of particles, and a second one, where $k_{\parallel}^2 < 0$ and absorption is due to excitation and also pair creation. In the present study we are going to use the expression of $\text{Im}[t]$ in the region of $k_{\parallel}^2 < 0$ because we will take the long wavelength limit ($k_3 \rightarrow 0$). Furthermore, only the region of real frequencies, which means, $k_3^2 > k_{\parallel}^2$ is considered. To find the imaginary part of I_t the formulas (A38)-(A42) will be used, after that we have

² we have returned to the units \hbar and c for obtain this result.

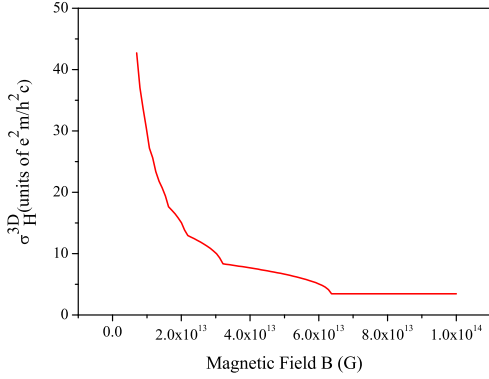


FIG. 1. (Color online) 3D Hall conductivity as a function of the magnetic field, where B runs between 7×10^{12} and 10^{14} G and $\hbar\omega = 10^{-2}$ MeV.

the Ohm conductivity as

$$\begin{aligned} \sigma_0^{3D}(\omega, B, \mu, T) &= \frac{Im[t]}{\omega} \\ &= \frac{e^3 B}{8\pi\omega} \sum_{nn'} \frac{F_{n,n'}^{(2)}(0)(k_{\parallel}^2 + 2eB(n+n'))}{((k_{\parallel}^2 + 2eB(n'-n))^2 + 4\varepsilon_{0,n}^2 k_{\parallel}^2)^{1/2}} \\ &\quad \times \left(\theta(k_{\parallel}^2 - k_{\parallel}^{2''}) \left[N(\varepsilon_p^{(m)}) - N(\varepsilon_p^{(m)} + \omega) \right] \right. \\ &\quad \left. + \theta(k_{\parallel}^{2'} - k_{\parallel}^2) \left[H(\varepsilon_p^{(j)}) + H(\omega - \varepsilon_p^{(j)}) - 2 \right] \right) \theta(k_3^2 - k_{\parallel}^2), \end{aligned} \quad (24)$$

where

$$\begin{aligned} N(\varepsilon_{p,n}) &= n_e(\varepsilon_{p,n}) + n_p(\varepsilon_{p,n}) \\ H(\varepsilon_{p,n}) &= n_e(\varepsilon_{p,n}) + n_p(\omega - \varepsilon_{p,n}). \end{aligned} \quad (25)$$

Equation (24) is written for $\omega > 0$, where $\varepsilon_p^{(m)}$ and $\varepsilon_p^{(j)}$ are the values of the energy at the branching points for the excitation and pair creation absorption processes respectively,

$$\begin{aligned} \varepsilon_p^{(m)} &= \frac{-\omega J_{nn'} \pm k_3 \Lambda}{2k_{\parallel}^2}, \quad m = (1, 2), \\ \varepsilon_p^{(j)} &= \frac{\omega J_{nn'} \mp k_3 \Lambda}{2k_{\parallel}^2}, \quad j = (3, 4) \end{aligned} \quad (26)$$

The step function over k_{\parallel}^2 in Eq. (24) defines the regions where excitation and pair creation take place, where $k_{\parallel}^{2'}$ and $k_{\parallel}^{2''}$ are the branching points located at k_{\parallel}^2 plane

$$k_{\parallel}^{2'} = -(\varepsilon_{0,n} + \varepsilon_{0,n'})^2, \quad k_{\parallel}^{2''} = -(\varepsilon_{0,n} - \varepsilon_{0,n'})^2. \quad (27)$$

Now, our attention is focused in the long wavelength and degenerate limit, in order to get a better understanding of our results, we separate them for each region.

a) Region I: $k_{\parallel}^2 > k_{\parallel}^{2''}$ excitation case.

In this region absorption occurs due to only the excitation of particles to higher energy levels. As $k_3 \rightarrow 0$, then $k_{\parallel}^2 = -\omega^2$. The solution for the energy are: $\varepsilon_p^{(1)} = \varepsilon_p^{(2)} = J_{nn'}/2\omega$. In order to have positive energies, which could be important in the degenerate limit, the sum is restricted to $n' > n$. Also, the condition $k_{\parallel}^2 > k_{\parallel}^{2''}$, in this limit, implies $2eB > \omega^2$. Finally, considering the degenerate limit, the Ohm conductivity in I is given by

$$\begin{aligned} \sigma_0^{3D}(\omega, B, \mu, 0) &= \frac{e^3 B}{8\pi\omega} \sum_{n=0}^{n_{max}} \frac{2eB(2n+1) - \omega^2}{((2eB - \omega^2)^2 - 4\varepsilon_{0,n}^2 \omega^2)^{1/2}} \\ &\quad (\theta(\mu - \varepsilon_p^{(1)}) - \theta(\mu - \varepsilon_p^{(1)} - \omega)). \end{aligned} \quad (28)$$

The sum over the integer n goes to n_{max} determined by the restriction imposed by Eq. (27). The combination of the degenerate functions tells us that the Ohm conductivity does not vanish if

$$\frac{2eB - \omega^2}{2\omega} < \mu < \frac{2eB + \omega^2}{2\omega}$$

b) Region II: $k_{\parallel}^{2'} > k_{\parallel}^2$ pair creation.

In this region absorption may be due to excitation and also to pair creation. The corresponding solution for the energies are: $\varepsilon_p^{(3)} = \varepsilon_p^{(4)} = -J_{nn'}/2\omega$. In this case there is no restriction for the sum over n , and the condition $k_{\parallel}^{2'} > k_{\parallel}^2$, implies $2eB < \omega^2$. Then, the expression for the Ohm conductivity in the degenerate limit in II is

$$\begin{aligned} \sigma_0^{3D}(\omega, B, \mu, 0) &= \frac{e^3 B}{8\pi\omega} \sum_{n=0}^{n_{max}} \frac{\omega^2 - 2eB(2n+1)}{((2eB - \omega^2)^2 - 4\varepsilon_{0,n}^2 \omega^2)^{1/2}} \\ &\quad + \sum_{n=1}^{\infty} \frac{\omega^2 - 2eB(2n-1)}{(2eB + \omega^2)^2 - 4\varepsilon_{0,n}^2 \omega^2)^{1/2}} (\theta(\varepsilon_p^{(3)} - \mu) + \theta(\omega - \varepsilon_p^{(3)} - \mu)), \end{aligned} \quad (29)$$

and from the degenerate distribution, we obtained that the Ohm conductivity does not vanish if

$$\frac{\omega^2 + 2eB}{2\omega} > \mu \quad \text{or} \quad \frac{\omega^2 - 2eB}{2\omega} > \mu. \quad (30)$$

Let us remark that in the static limit, $\omega = 0$ the Ohm conductivity is zero as was checked in Ref. [20].

III. QUANTUM FARADAY EFFECT FOR A RELATIVISTIC FERMION GAS

Photons propagating in a relativistic fermion-antifermion (e^\pm) medium at zero temperature and nonzero particle density (chemical potential μ) is of special interest for astrophysics. The one-loop diagram describing the process accounting for the photon self-energy interaction contains, in addition to the virtual creation and annihilation of the pair, the process of absorption and subsequent emission of one photon by the fermions and/or antifermions.

The propagation of an electromagnetic wave in the medium can be described by the Maxwell equations

$$\partial_\nu F_{\nu\mu} + \Pi_{\mu\nu} a_\nu = 0, \quad (31)$$

which could be written in momentum space as

$$\left[(k_\perp^2 + k_\parallel^2) g_{\mu\nu} - k_\mu k_\nu + \Pi_{\mu\nu} \right] a_\nu = 0, \quad (32)$$

We will consider in what follows that the photon propagates parallel to the magnetic field. As in Sec. II, $\Pi^{\nu\rho}$ is the self-energy of the photon propagating in a magnetized dense medium, so it depends on T , μ , and magnetic field, apart from k_3 and ω .

To solve the dispersion relation (32) we need to diagonalize $\Pi_{\nu\rho}$. The general covariant structure of the photon self-energy leads to the following expression:

$$\Pi_{\mu\nu} = \sum_{n=0}^3 \kappa_i \frac{b_{\mu^{(i)}} b_{\nu}^{*(i)}}{b_{\mu}^{(i)} b_{\mu}^{*(i)}}, \quad \nu, \mu = 1, 2, 3, 4. \quad (33)$$

where κ_i and $b_{\mu}^{(i)}$ are the eigenvalues and the eigenvectors of $\Pi_{\mu\nu}$, respectively, which satisfies the secular equation

$$\Pi_{\mu\nu} b_{\nu}^{(i)} = \kappa_i b_{\mu}^{(i)}. \quad (34)$$

In the particular case of propagation along the magnetic field there are three nonvanishing eigenvalues.

The first two are transverse modes $b_{\mu}^{(1,2)}$ [5]-[2] (see appendix for details).

$$b_{\mu}^{(1,2)} = (b_{\mu}^{(1)} \pm i b_{\mu}^{(2)}), \quad (35)$$

$$\text{with } \vec{b}_{\perp}^{(1)} = -\frac{\vec{k}_{\perp}}{k_{\perp}} \frac{k_{\parallel}}{k}, \quad b_{3,0}^{(1)} = 0,$$

$$b_1^{(2)} = \frac{k_2}{k_{\perp}}, \quad b_2^{(2)} = -\frac{k_1}{k_{\perp}}, \quad b_{3,0}^{(2)} = 0, \quad (36)$$

which describe a circularly polarized wave in the plane perpendicular to \mathbf{B} with different eigenvalues,

$$\kappa_{1,2} = t \pm \sqrt{-r^2}, \quad (37)$$

according to the definition given in Eq. (11),

$$\kappa_{1,2} = t \pm I_r, \quad (38)$$

that is, opposite directions, which is the key of the Faraday effect. Also, there is a third mode corresponding to a longitudinal wave which propagates along the magnetic field b_{μ}^3 , and $\kappa_3 = s$ is the corresponding eigenvalue.

Let us consider the propagation of an electromagnetic wave, which at $x_3 = 0$ is linearly polarized along the x_1 axes. Note that, because the system has rotational symmetry with regard to \mathbf{B} ($k_{\perp} = 0$), we can choose the direction of the eigenvectors $b_{\mu}^{1,2}$ arbitrarily orthogonal to \mathbf{B} . We can then set $\frac{\vec{k}_{\perp}}{k_{\perp}} = \mathbf{e}_1$, and decompose the wave into two circularly polarized waves

$$a_{\mu} = \left[\frac{1}{2} A e^{i(k+x_3-\omega t)} b_{\mu}^{(1)} + \frac{1}{2} A e^{i(k-x_3-\omega t)} b_{\mu}^{(2)} \right], \quad (39)$$

where k_{\pm} are the solutions of the dispersion relations for the eigenmodes

$$k_{\pm} = \sqrt{\omega^2 + \kappa_{1,2}} = \sqrt{\omega^2 + t \pm I_r}, \quad (40)$$

In order to solve the dispersion relation, the complex functions r and t in (40) are considered in an approximation independent on k_3 (35).

The electric field associated with the wave is given by

$$\mathbf{E} = \left[\frac{i\omega}{\sqrt{2}} A e^{i(k+x_3-\omega t)} \mathbf{e}^+ + \frac{i\omega}{\sqrt{2}} A e^{i(k-x_3-\omega t)} \mathbf{e}^- \right], \quad (41)$$

where $\mathbf{e}^{\pm} = (\mathbf{e}_1 \mp i\mathbf{e}_2)/\sqrt{2}$ are the polarization vectors of the left and right circularly polarized waves, respectively. So, the superposition of both modes leads to

an elliptically polarized wave, whose principal axis rotate.

The amount of the FR angle, after traveling a distance L in the medium, can be obtained from (see also Refs. [21]-[22])

$$\theta_F^{3D} = \frac{1}{2}\omega(n_- - n_+)L, \quad (42)$$

where n_{\pm} are the refraction indices of the left- and right-circularly polarized waves, respectively, and can be defined as [2]

$$n_{\pm}(\omega, k_3) = (1 + \frac{\kappa_{1,2}(\omega, k_3)}{\omega^2})^{1/2}. \quad (43)$$

Using $k = n\omega$, then the Faraday angle can be obtained directly from Eqs. (41) and (42):

$$\theta_F^{3D} = \frac{1}{2}(Re[k_-] - Re[k_+])L, \quad (44)$$

where

$$Re[k_{\pm}] = \frac{1}{\sqrt{2}} \sqrt{(\omega^2 + Re[\kappa_{1,2}])^2 + Im[\kappa_{1,2}]^2 + (\omega^2 + Re[\kappa_{1,2}])^2}^{1/2}. \quad (45)$$

If $Im[\kappa_{1,2}] \ll \omega^2 + Re[\kappa_{1,2}]$ we can roughly write

$$Re[k_{\pm}] \approx \sqrt{\omega^2 + Re[\kappa_{1,2}]} \left[1 + \frac{Im[\kappa_{1,2}]^2}{4(\omega^2 + Re[\kappa_{1,2}])^2} \right]^{1/2}. \quad (46)$$

Furthermore, if also $Re[\kappa_{1,2}] \ll \omega^2$, in the leading-order approximation

$$Re[k_{\pm}] \approx \omega + \frac{Re[\kappa_{1,2}]}{2\omega}, \quad (47)$$

and, according to the relation given in Ref. (44), we obtain for the rotated Faraday angle per unit length³

$$\frac{\theta_F^{3D}}{L} \sim \frac{\sigma_H^{3D}}{2c}. \quad (48)$$

Equation (48) shows the relation between Faraday angle and the Hall conductivity. Let us note that in general the Faraday angle depends on the terms of the admittivity tensor but the leading term comes from the Hall conductivity. This result obtained for 3D+1 systems shows that it is a consequence of general properties of QED in an external magnetic field at finite

density. In Sec. V we have obtained in 2D+1 limit. This result has been obtained theoretically in 2D+1 systems [12], [13], [24].

The Faraday angle in the degenerate limit (σ_H^{3D} is given by Eq. (22)) has been depicted in Fig. 2, for $n_{\mu} = 0$ in a wide range of photon energy. Because the Hall conductivity (22) has two branching points for $n_{\mu} = 0$, the curve has two peaks related to excitation ($\omega = -m + (m^2 + 2eB)^{1/2}$) and pair creation ($\omega = m + \sqrt{m^2 + 2eB}$). Then a resonant behavior for the Faraday angle is obtained, associated with both absorption processes [5]. Let us note that the Faraday angle should be a finite value. The divergences are avoided if we use the solution of the dispersion equation near the singular points.

The relativistic quantized medium makes the angle depend nonlinearly on the magnetic field, contrary to the classical case of interstellar medium where the relation with B is linear and depends on the electron density.

It is worthwhile to point out that Faraday effect is obtained as the consequence of charge asymmetry of the system $\mu \neq 0$. When the system has charge symmetry the scalar r vanishes and the Faraday effect is not manifested.

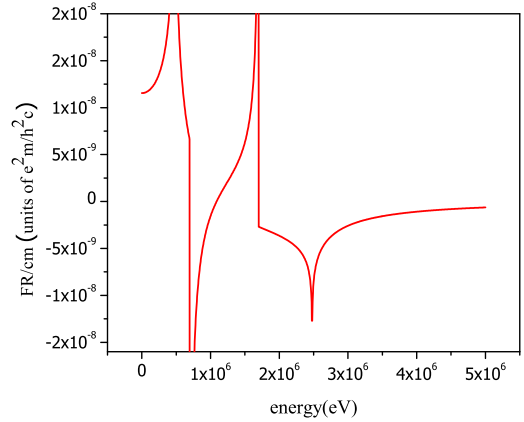


FIG. 2. (Color online) Faraday angle per unit length as a function of energy, for $\mu = 1$ MeV and $B = 10^{14}$ G, corresponding to n_{μ} . The curve was plotted in a wide range of the photon energy $\hbar\omega = [10^2 - 5 \times 10^6] \text{ eV}$ which includes the two branching points for the FR

³ We have returned to the units \hbar and c to obtain this result.

IV. RELATIVISTIC HALL AND OHM CONDUCTIVITIES IN NON-STATIC LIMIT ($\omega \neq 0$: 2D+1 SYSTEM)

As is well known theoretically properties of graphene are essentially described by Dirac massless fermions (electrons) in two dimensions. This system is “relativistic” in the sense that the spectra of electrons and holes can be mimicked as two-dimensional relativistic chiral fermions where electrons and holes move at velocities $v_F \approx 10^6 m/s$ one hundredth the speed of light [8]. In this section with the aim of studying a graphene like system we are going to obtain the 2D Hall and Ohm conductivities in the nonstatic limit from the 3D conductivities obtained in Sec. II. Two considerations can be made: the first is to do a dimensional compactification [10],[20] and the second one is to take the limit $m \rightarrow 0$ [10]. To consider the first of our assumptions, we assume that the fermion-antifermion gas is confined to a box of length L_3 and the limit $L_3 \rightarrow 0$ is taken. Then the integral over p_3 is replaced by a sum over the integers $s = 0, 1, 2, \dots$. Because $p_3 = 2\pi s/L_3$ and $L_3 \rightarrow 0$ only the terms $s = 0$ remain in the sum. Then the 2D+1 limit is obtained taking $p_3 = 0$ and $k_3 = 0$ and removing from all the expressions the integrals $1/(2\pi\hbar) \int dp_3$. With this dimensional reduction and the consideration of massless fermions in mind for 2D+1 Hall conductivity at $\omega \neq 0$,

we have ($Y_{ij}^{2D} = L_3 Y_{ij}$)

$$\sigma_H^{2D}(\omega, B, \mu, T) = \frac{Im[r^{2D}(\omega, B, \mu, T)]}{\omega} L_3, \quad (49)$$

and

$$\sigma_H^{2D} = \frac{e^3 B}{\pi} \sum_{n=0}^{\infty} \left(\frac{(-\omega^2 + 2eB(2n+1))}{(-\omega^2 + 2eB)^2 - 4\omega^2 \varepsilon_{0,n}^2} - \sum_{n=1}^{\infty} \frac{-\omega^2 + 2eB(2n-1)}{(\omega^2 + 2eB)^2 - 4\omega^2 \varepsilon_{0,n}^2} \right) (n_e - n_p), \quad (50)$$

where $\varepsilon_{0,n} = \sqrt{2neB}$. As in the earlier section we consider the zero-temperature limit which means substituting $n_e(\varepsilon) = \theta(\mu - \varepsilon)$ and zero contribution of antifermions, since the gas is completely degenerate. The Hall Conductivity has been written as

$$\sigma_H^{2D}(\omega, B, \mu, 0) = \frac{e^3 B}{\pi} \left\{ \frac{-\omega^2 + 2eB(2n_\mu + 1)}{(2eB - \omega^2)^2 - 4\omega^2 \varepsilon_{0,n_\mu}^2} \right\}. \quad (51)$$

Let us remark that at $\omega = 0$ we recover the expression of quantum Hall Conductivity $\sigma_H^{2D} = 2\frac{e^2}{h}(n_\mu + \frac{1}{2})$.⁴ The Ohm conductivity should be obtained doing the dimensional reduction in Eq. (15) considering massless fermions. In the degenerate limit, we obtain

$$\sigma_0^{2D}(\omega, B, \mu, 0) = \frac{e^3 B}{2\pi\omega} \sum_{n=0}^{n_\mu} \varepsilon_{0,n} \left(\frac{2\omega^2 + 4eB}{((-\omega^2 + 2eB)^2 - 4\omega^2 \varepsilon_{0,n}^2)} + \frac{2\omega^2 - 4eB}{((\omega^2 + 2eB)^2 - 4\omega^2 \varepsilon_{0,n}^2)} \right) \theta(\mu - \varepsilon_{0,n}), \quad (52)$$

Let us note that in Eq. (52) the sum over n goes to $n_\mu = I[\frac{\mu^2}{2eB}]$.

Although our method of dimensional reduction described above is valid for getting 2D+1 limits, it would be interesting to make a full 2D+1 analysis of the problem by discussing the set of independent tensor structures involved and their relation to the obtained results. Reference [25] is an early attempt to deal with the 2D+1 case related to the Chern-Simons addition to the Lagrangian.

To consider a graphene-like system in Eqs. (51) and (52), additional considerations must be taken into account. When the units \hbar and c are recovered, $c \rightarrow v_f^2/c$ (v_f is the Fermi velocity)[10]. The expressions for the Hall and Ohm conductivities [Eqs. 51)-(52] must be multiplied by two, to account for the sublattice-valley degeneracy in graphene. The frequency must be substituted by $\omega \rightarrow \omega + i\epsilon$ where the imaginary part- ϵ is a phenomenological parameter associated with system disorder ([13],[14]). In Fig. 3 the 2D Ohm conductivity is plotted as a function of energy for fixed values of $B = 7 \times 10^4$ G, chemical potential $\mu = 200$ MeV and $\epsilon = 6.8$ MeV, which are typical values for a graphene-like system [14] and [13]. The figure also shows the

⁴ we have recovered the units \hbar and c to write this result.

imaginary part of the conductivity. Our results obtained with the *ansatz* of a dimensional compactification are in agreement with the theoretical studies of the Ohm conductivity in graphene [14],[16].

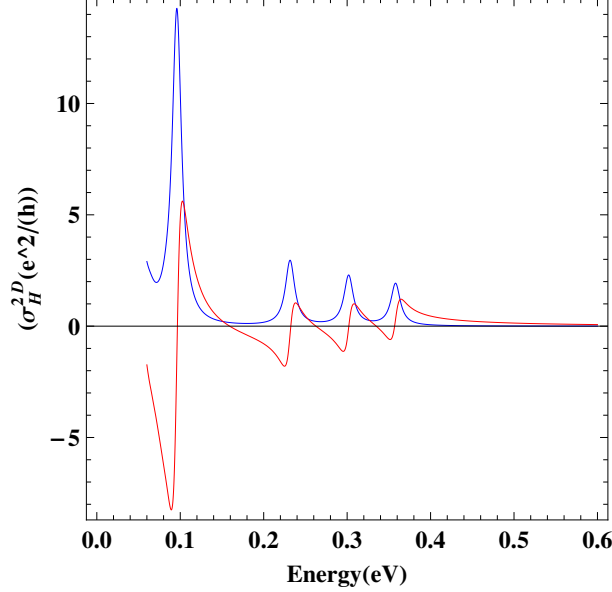


FIG. 3. (Color online) Ohm Conductivity (solid blue line) as a function of the photon energy for $B = 7 \times 10^4$ G, $\mu = 200$ MeV and $\epsilon = 6.8$ MeV. We use $v_f = 10^8$ cm/s. We also have plotted the imaginary part of the conductivity (dashed red line).

V. 2D+1 SYSTEM: FARADAY EFFECT AND ROTATION FARADAY ANGLE

The purpose of this section is to study the Faraday effect for a 2D+1 system (i.e., a graphene like system) starting from the results obtained in Sec. III. Let us suppose that the graphene plate is located at $x_3 = 0$ and the incoming electromagnetic wave is linearly polarized along the x_1 direction, and travels in the positive x_3 direction. Due to the optical Faraday rotation of the polarization vector when the wave crosses the graphene sheet, both the reflected and transmitted component acquire a component along the x_2 direction ([13],[14],[26]).

We can formally follow the procedure of by III by using the solution of the dispersion relation for a photon in a stratified medium, given by a 3D+1 relativistic electron-positron plasma, situated between $x_3 = 0$ and $x_3 = L_3$, in vacuum.

To describe the propagation of an electromagnetic wave in the whole space, let us start from the modified Maxwell Eq. (31) as

$$\partial_\nu F^{\nu\mu} + (\theta(x_3) - \theta(x_3 - L_3))\Pi_{\mu\nu}a_\nu = 0 \quad (53)$$

where the θ -functions account for the inhomogeneity in the Maxwell equation, which is only at $0 < x_3 < L_3$. The boundary conditions at the medium surfaces imply the continuity of the electric field

$$E^i(x_3 = 0-, L_3-) = E^i(x_3 = 0+, L_3+) \quad (54)$$

and its derivatives

$$\partial_3 E^i(x_3 = 0-, L_3-) = \partial_3 E^i(x_3 = 0+, L_3+). \quad (55)$$

If we consider an incident electromagnetic wave linearly polarized along the x_3 direction,

$$\mathbf{E}^I = \frac{E}{\sqrt{2}} e^{i(kx_3 - \omega t)} \mathbf{e}^+ + \frac{E}{\sqrt{2}} e^{i(kx_3 - \omega t)} \mathbf{e}^-, \quad (56)$$

the transmitted wave ($x_3 > L_3$) can be written as

$$\mathbf{E}^T = \frac{E^+}{\sqrt{2}} e^{i(kx_3 - \omega t)} \mathbf{e}^+ + \frac{E^-}{\sqrt{2}} e^{i(kx_3 - \omega t)} \mathbf{e}^-, \quad (57)$$

where $E_\pm = (E_1 \pm iE_2)$ are complex amplitudes and $\mathbf{e}^\pm = (\mathbf{e}_1 \mp i\mathbf{e}_2)/\sqrt{2}$ correspond to the left- and right-polarized waves, respectively [27]. In order to express the amplitudes E_\pm in terms of the medium parameters and the amplitude of the incident wave E , we can follow the multiple-reflections method described in Ref. [28]. Let us define the complex total transmission coefficients amplitudes $T_\pm = E_\pm^T/E_\pm^I$,

$$T_\pm = \frac{\tau_\pm e^{ik_\pm L_3}}{1 + \varrho_\pm e^{2ik_\pm L_3}}, \quad (58)$$

where the factors $\tau_\pm = \frac{4kk^\pm}{(k^\pm + k)^2}$, and $\varrho_\pm = \frac{(k^\pm - k)^2}{(k^\pm + k)^2}$ come from the boundary conditions (54) and (55) and the exponentials $e^{ik_\pm L_3}$ are related to the FR due to the propagation in the medium (as was shown in detail in Sec. III). Because T_\pm are complex numbers, they can be written as $T_\pm = |T_\pm|e^{i\theta_\pm}$, and using the definition given above for the Faraday angle [Eq. 44]

$$\theta_F = \frac{1}{2}(\theta_- - \theta_+). \quad (59)$$

In the limit case $k_\pm L_3 \ll 1$, we can expand the exponentials in (58) up to the linear term in L_3 , and obtain the approximate expressions

$$T_\pm \approx \frac{1}{1 - iL_3 \frac{k_\pm^2 + k^2}{2k}} = \frac{2}{1 + L_3 \frac{\kappa_{1,2}}{i\omega} - iL_3 \omega}. \quad (60)$$

Finally, when $L_3 \rightarrow 0$, $L_3 \frac{\kappa_{1,2}}{i\omega} \rightarrow Y_{\pm} = Y_{11}^{2D} \pm iY_{12}^{2D}$, where Y_{ij}^{2D} are the components of the 2D complex conductivity tensor, obtained from the 3D ones by the dimensional reduction prescription described in the previous section. The Faraday angle in the 2D+1 limit is then given by

$$\theta_F^{2D} = \frac{1}{2}(\theta_-^{2D} - \theta_+^{2D}), \quad (61)$$

where $\theta_{\pm}^{2D} = \arg[T_{\pm}^{2D}]$ and

$$T_{\pm}^{2D} = \frac{2}{2 + Y_{\pm}}. \quad (62)$$

It is easy to see from the last two equations that, in the leading order approximation,

$$\theta_F^{2D} = \frac{1}{2}\sigma_H^{2D}. \quad (63)$$

This relation between the Faraday angle and the Hall Conductivity has been already obtained in graphene [11], [13],[14] and here we have obtained it naturally from the 3D result after a dimensional compactification.

It can be easily checked that our approach is equivalent to the one followed in Ref. [13] by taking the limit $L_3 \rightarrow 0$ in Eq. (53).

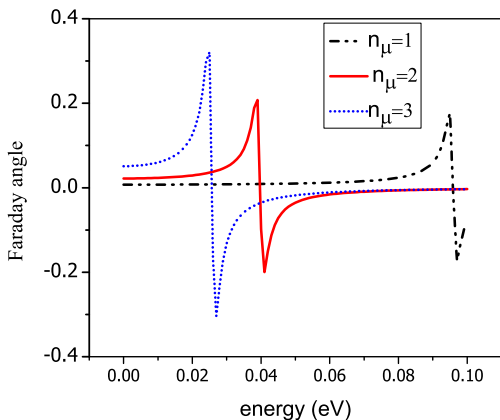


FIG. 4. (Color online) Faraday angle as a function of the energy for $B = 7 \times 10^4$ G, $\epsilon = 1$ MeV and three different values of the chemical potential: $\mu = (30, 110, 180)$ MeV

The Faraday angle is plotted in Figs. (4) and (5) in the degenerate limit [in which Hall conductivity is given by Eq. (51)]. Figure (4) shows the Faraday

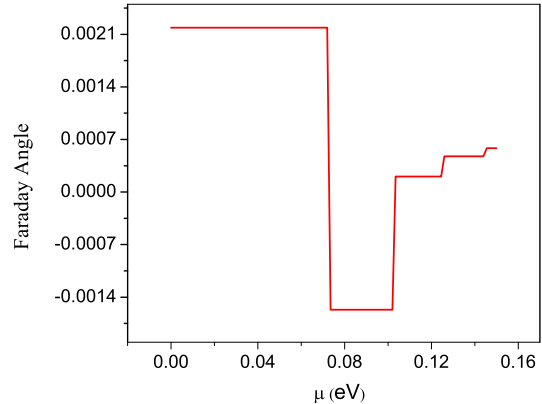


FIG. 5. (Color online) Faraday angle as a function of the chemical potential for $B = 4 \times 10^4$ G, $\hbar\omega = 150$ MeV and $\epsilon = 0.5$ MeV. We use $v_f = 10^8$ cm/s.

rotation angle versus ω for a fixed value of the magnetic field 7×10^4 G and maximum Landau numbers $n_{\mu} = 0, 1, 3$, which corresponds to chemical potentials $\mu = (30, 110, 180)$ MeV, respectively. Each curve shows peaks associated with the poles of the Hall conductivity (51) showing a resonant behavior for the Faraday angle when the frequency reaches the values corresponding to the poles and absorption processes occurs. The curves were done assuming $\epsilon = 1$ MeV which is a typical value of this quantity in graphene-like systems. The maximum rotation angle for the parameters chosen is in agreement with the angle predicted by Ref. [15]. In Fig. 5 the Faraday angle is plotted as a function of chemical potential fixing $B = 4 \times 10^4$ G, $\hbar\omega = 150$ MeV and $\epsilon = 0.5$ MeV. The curve shows a quantized behavior in the same way as the Hall conductivity.

VI. CONCLUSIONS

The study of propagation of an electromagnetic wave parallel to a magnetic field has been done starting from quantum field theory formalism at finite temperature and density. The quantum Faraday effect has been studied in 3D+1 and 2D+1 systems. We have obtained the relation between the FR angle and Hall Conductivity (the Faraday angle is given by the complex conductivity, but the leading term comes from the Hall conductivity). Our finding shows that it is a consequence of general properties of propagation of an

electromagnetic wave parallel to a constant magnetic field, in a quantum and relativistic dense system. We have found that Faraday effect is consequence of the C noninvariance of the system.

Due to the relation between Faraday effect and Hall conductivity we started our calculations studying the conductivity tensor in the nonstatic limit. Hall and Ohm conductivities have been calculated in the limit of zero temperature relevant for applications to astrophysical and graphene-like systems. The calculations can be extended to the general case of finite temperature.

Let us remark that in the present paper we have focused on the real Ohm and Hall conductivities given by the imaginary part of t and the principal value of the integral I_r , respectively. A more full discussion of the complex conductivity including for instance the imaginary part of integral I_r (related to absorptive processes) and the real part of t will be discussed in a separate work.

The 2D+1 quantum relativistic system has also been studied by introducing the ansatz of dimensional compactification of the x_3 dimension, allowing us to obtain the Hall and Ohm conductivities in the limit of zero temperature.

The Faraday angle shows a quantized behavior in both 3D+1 and 2D+1 relativistic system. The dependence of the Faraday angle with frequency in graphene-like system is in agreement with theoretical studies [13]-[14]. Giant Faraday angles are found for photon absorption frequencies. The outcome related to the Faraday rotation angle in the astrophysical context, in particular in the study of propagation of light in the magnetosphere of neutron stars, deserves to be carefully analyzed. A separate study of this topic will

be addressed in a future work.

ACKNOWLEDGMENTS

The authors thanks to A. Cabo and A. Gonzalez Garcia for fruitful discussions. This work has been supported under the grant CB0407 and the ICTP Office of External Activities through NET-35.

Appendix A: Properties of the photon self-energy tensor

As a starting point we summarize some of the main features related with the photon self-energy of an electron-positron plasma in the presence of a constant magnetic field in the case of nonzero temperature and

nonvanishing chemical potential. Under these conditions the polarization tensor may be expanded in terms of six independent transverse tensors [5]. As is shown in Ref. [2], symmetric properties in quantum statistics, corresponding to generalization of the Onsager relations, reduce the number of the basic tensors from 9 to 6:

$$\Pi_{\mu\nu} = \sum_{n=1}^6 \pi^{(n)} \Psi_{\mu\nu}^{(n)}, \quad \nu, \mu = 1, 2, 3, 4 \quad (\text{A1})$$

The basic tensors are

$$\Psi_{\mu\nu}^{(1)} = k^2 g_{\mu\nu} - k_\mu k_\nu, \quad \Psi_{\mu\nu}^{(2)} = F_{\mu\lambda} k^\lambda F^{\nu\rho} k_\rho, \quad (\text{A2})$$

$$\Psi_{\mu\nu}^{(3)} = -k^2 (g_{\mu\nu} - \frac{k_\mu k_\nu}{k^2}) F_\rho^\lambda F^{\rho\eta} (g_{\eta\nu} - \frac{k_\eta k_\nu}{k^2}), \quad (\text{A3})$$

$$\Psi_{\mu\nu}^{(4)} = \frac{-[(F^2 k)_\mu k^2 - k_\mu (k F^2 k)](F^* k)_\nu + (F^* k)_\mu [(F^2 k)_\nu k^2 - k_\nu (k F^2 k)]}{(k F^{*2} k)[-k^2((k F^2 k))]^{1/2}}, \quad (\text{A4})$$

where $g_{\mu,\nu} = (-1, 1, 1, 1)$ is the metric tensor and $F_{\mu\nu}^*$ is the dual of the electromagnetic tensor $F_{\mu,\nu}$.

These tensors are symmetric in the indexes μ, ν while the following ones are antisymmetric

$$\Psi_{\mu\nu}^{(5)} = (u \cdot k)(k_\mu F_{\mu\lambda} k^\lambda - k_\nu F_{\mu\lambda} k^\lambda + k^2 F_{\mu\nu}), \quad (\text{A5})$$

$$\Psi_{\mu\nu}^{(6)} = u_\lambda F_{\mu\lambda} k^\lambda - u_\nu F_{\mu\lambda} k^\lambda - (u \cdot k) F_{\mu\nu}. \quad (\text{A6})$$

We introduce a set of orthonormal vectors which are the eigenvectors of $\Pi_{\mu\nu}$ in the limit $\mu = 0$ and $\beta^{-1} = 0$

$$b_\mu^{(1)} = \frac{(F^2 k)_\mu k^2 - k_\mu (k F^2 k)}{(-k^2 (k F^2 k)(k F^{*2} k))^{1/2}}, \quad (\text{A7})$$

$$b_\mu^{(2)} = \frac{(F^* k)_\mu}{(k F^{*2} k)^{1/2}}, \quad (\text{A8})$$

$$b_\mu^{(3)} = \frac{(F k)_\mu}{(-k F^2 k)^{1/2}}, \quad (\text{A9})$$

$$b_\mu^{(4)} = \frac{k_\mu}{(k^2)^{1/2}}. \quad (\text{A10})$$

In the reference system in which the electron positron plasma is at rest, the vectors $b_\mu^{(i)}$ look like

$$\vec{b}_\perp^{(1)} = -\frac{\vec{k}_\perp}{k_\perp} \sqrt{\frac{k_\parallel^2}{k^2}}, \quad b_{3,0}^{(1)} = k_{3,0} \sqrt{\frac{k_\perp^2}{k_\parallel^2 k^2}}, \quad (\text{A11})$$

$$\vec{b}_\perp^{(2)} = 0, \quad b_3^{(2)} = \frac{k_0}{\sqrt{k_\parallel^2}}, \quad b_0^{(2)} = \frac{k_3}{\sqrt{k_\parallel^2}}, \quad (\text{A12})$$

$$b_1^{(3)} = \frac{k_2}{\sqrt{k_\perp^2}}, \quad b_2^{(3)} = -\frac{k_1}{\sqrt{k_\perp^2}}, \quad b_{3,0}^{(3)} = 0, \quad (\text{A13})$$

$$b_\mu^{(4)} = \frac{k_\mu}{(k^2)^{1/2}}. \quad (\text{A14})$$

Using these vectors we can derive the scalars

$$p = b^{(1)\mu} \Pi_\mu^\nu b_\nu^{(1)}, \quad (\text{A15})$$

$$s = b^{(2)\mu} \Pi_\mu^\nu b_\nu^{(2)}, \quad (\text{A16})$$

$$t = b^{(3)\mu} \Pi_\mu^\nu b_\nu^{(3)}, \quad (\text{A17})$$

$$r = b^{(3)\mu} \Pi_\mu^\nu b_\nu^{(1)}, \quad (\text{A18})$$

and the pseudoscalar

$$q = b^{(2)\mu} \Pi_\mu^\nu b_\nu^{(1)}, \quad (\text{A19})$$

$$v = b^{(2)\mu} \Pi_\mu^\nu b_\nu^{(3)}. \quad (\text{A20})$$

In terms of this quantities the scalars $\pi^{(i)}$ in Eq. A1 may be written in the rest frame ($u_\nu = (0, 0, 0, 1)$) as

$$\pi^{(1)} = s/k^2, \quad (\text{A21})$$

$$\pi^{(2)} = (k_\parallel^2 t - k^2 p + k_\perp^2 s)/B^2 k_\parallel^2 k_\perp^2, \quad (\text{A22})$$

$$\pi^{(3)} = (p - s)/B^2 k_\parallel^2, \quad \pi^{(4)} = q, \quad (\text{A23})$$

$$\pi^{(5)} = -\frac{r}{B\omega(k^2 k_\parallel^{1/2})} - \frac{v}{Bk_3(k_\parallel^2 k_\perp^2)^{1/2}}, \quad (\text{A24})$$

$$\pi^{(6)} = \frac{v}{Bk_3} \frac{k_\parallel}{k_\perp}. \quad (\text{A25})$$

The above expression were written taking into account that the magnetic field is directed along the x_3 axis. Then, $\Pi_{\mu\nu}$ can be expressed in terms of the base

vectors b_ν^i :

$$\Pi_\mu^\nu b_\nu^{(1)} = p b_\mu^{(1)} + q b_\mu^{(2)} + r b_\mu^{(3)}, \quad (\text{A26})$$

$$\Pi_\mu^\nu b_\nu^{(2)} = -q b_\mu^{(1)} + s b_\mu^{(2)} + v b_\mu^{(3)}, \quad (\text{A27})$$

$$\Pi_\mu^\nu b_\nu^{(3)} = -r b_\mu^{(1)} + v b_\mu^{(2)} + t b_\mu^{(3)}, \quad (\text{A28})$$

$$\Pi_\mu^\nu b_\nu^{(4)} = 0. \quad (\text{A29})$$

Finally the polarization tensor can be expressed in the $b_\nu^{(i)}$ base as

$$\Pi_{\mu\nu} = \begin{bmatrix} p & q & r \\ -q & s & v \\ -r & v & t \end{bmatrix}. \quad (\text{A30})$$

From these results the eigenvalues could be determined by finding the modes of the wave propagating in the medium. In the case of propagation along the magnetic field, $k_\perp = 0$, we obtain $q = v = 0$ and $p = t$ and Eq. (A30) becomes

$$\Pi_{\mu\nu} = \begin{bmatrix} t & 0 & r \\ 0 & s & 0 \\ -r & 0 & t \end{bmatrix}, \quad (\text{A31})$$

with the eigenmodes $b'^{(1,3)} = b^{(1)} \pm i b^{(3)}$ and $b'^{(2)} = b^{(2)}$ and eigenvalues $\kappa^{(1,3)} = t \pm \sqrt{-r^2}$ and $\kappa^{(2)} = s$. Equation (A31) is equivalent to

$$\Pi_{\mu\nu} = \begin{bmatrix} t & r & 0 \\ -r & t & 0 \\ 0 & 0 & s \end{bmatrix}, \quad (\text{A32})$$

and the eigenmodes $b_\mu'^{(1,2)} = b_\mu^{(1)} \pm i b_\mu^{(2)}$ and $b_\mu'^{(3)} = b_\mu^{(3)}$ and eigenvalues $\kappa_{1,2} = t \pm \sqrt{-r^2}$ and $\kappa_3 = s$.⁵

On the other hand, it follows from Eq. (A32) that we can calculate the scalars r and tt , which are given as

$$r(k|A; \mu, \beta^-) = -\frac{e^3 B}{2\pi^2 \beta} \sum_{p_4} \sum_{n, n'} \int_{-\infty}^{\infty} \frac{dp_3 C_{12, 21}}{(p_4'^2 + \varepsilon_p^2)((p_4' + k_4)^2 + \varepsilon_p^2)}, \quad (\text{A33})$$

where $C_{12, 21} = \pm i[p_4(p_4' + k_4) + p_3(p_3' + k_3) + m^2]F_{n, n'}^3$ and $F_{n, n'}^3(\frac{k^2}{eB}) = |T_{n-1, n'-1}|^2 + |T_{n-1, n'}|^2$ and

$$t(k|A; \mu, \beta^-) = -\frac{e^3 B}{2\pi^2 \beta} \sum_{p_4} \sum_{n, n'} \int_{-\infty}^{\infty} \frac{dp_3 C_{11, 22}}{(p_4'^2 + \varepsilon_p^2)((p_4' + k_4)^2 + \varepsilon_p^2)}, \quad (\text{A34})$$

and $C_{11, 22} = p_4[p_4(p_4' + k_4) + p_3(p_3' + k_3) + m^2]F_{n, n'}^2$ and $F_{n, n'}^2(\frac{z_2}{eB}) = |T_{n-1, n'-1}|^2 - |T_{n-1, n'}|^2$, with

$$T_{n,m}(p, y) = \int e^{ipy} \Psi_n(x) \Psi_m(x+y) dx = \left(\frac{m!}{n!}\right)^{1/2} \left(-\frac{y-ip}{\sqrt{2}}\right)^{n-m} e^{-ipy - \frac{p^2+y^2}{4}} L_m^{n-m}\left(\frac{p^2+y^2}{2}\right), \quad (\text{A35})$$

where L_m^{n-m} are the generalized Laguerre polynomials.

The sum \sum_{p_4} is done using the Matsubara formalism where we have

and the sum is carried out using the prescription

$$\frac{1}{\beta} \sum_n F\left(\dots \frac{2n\pi}{\beta}\right) = -\frac{1}{\beta} \sum_p f^\pm(\theta_p) \text{Res}\{F(\dots \theta_p)\}, \quad (\text{A37})$$

where $f^\pm = \pm \frac{i\beta}{1 - e^{\mp i\beta\theta}}$ and θ_p are the poles of F .

$$\int_{-\infty}^{\infty} \frac{dp_4}{2\pi} \rightarrow \frac{1}{\beta} \sum_{p_4}, \quad p_4 = \frac{(2n+1)\pi}{\beta}, \quad n = 0, \pm 1, \pm 2, \dots \quad (\text{A36})$$

1. Calculation of $Im[t]$, σ^0 in 3D+1: $k_{\parallel}^2 < 0$

In order to solve the integrals I_t and I_r which have singularities due to the denominator D , which can be written as

$$D^{-1} = \frac{1}{8\varepsilon_{n'}\varepsilon_n\omega} \left(\frac{1}{\varepsilon_{n'} - \varepsilon_n - \omega + i\epsilon} - \frac{1}{\varepsilon_{n'} - \varepsilon_n + \omega + i\epsilon} - \frac{1}{\varepsilon_{n'} + \varepsilon_n - \omega + i\epsilon} + \frac{1}{\varepsilon_{n'} + \varepsilon_n + \omega + i\epsilon} \right), \quad (\text{A38})$$

where we have added an infinitesimal positive imaginary part to ω , in order to take advantage of the relation

$$\frac{1}{s - \omega - i\epsilon} = P \frac{1}{s - \omega} + i\pi\delta(s - \omega), \quad (\text{A39})$$

to extract the imaginary and real part of the integrals. The first pair of singularities are related to excitation of particles to higher energies and the second two are connected to the pair creation. For $\varepsilon_{n'} > \varepsilon_n$ the first and the third of these denominators may vanish only for $\omega > 0$ and the second and fourth if $\omega < 0$. If $\varepsilon_{n'} < \varepsilon_n$ the opposite condition hold.

The imaginary part of the denominator D of the integrals (11) and (15) can be written as [5]

$$Im[D^{-1}] = \pm \frac{\pi}{8\varepsilon_n\varepsilon_{n'}\omega} (\delta(\varepsilon_{n'} - \varepsilon_n \mp \omega) + \delta(\varepsilon_{n'} - \varepsilon_n \pm \omega) - \delta(\varepsilon_{n'} + \varepsilon_n \mp \omega)), \quad (\text{A40})$$

To calculate the integral over p_3 we can use the formula

$$\int_{-\infty}^{\infty} dp_3 f(p_3) \delta(g(p_3)) = \sum_m \frac{f(p_3^m)}{|g'(p_3^m)|}, \quad (\text{A41})$$

⁵ Equation A32 corresponds to the Eq. (4.38) of Ref. [22]. The eigenvalues $\kappa_{1,2} = t \pm I_r$ are their $\pi_T \pm \pi_P$. The scalars t and I_r corresponds to π_T and π_P , respectively.

where p_3^m are the roots of $g(p_3) = 0$.

$$\left| \frac{d}{dp_3}(g(p_3)) \right| = \frac{\Lambda}{2\varepsilon_n^m \varepsilon_{n'}^m}. \quad (\text{A42})$$

-
- [1] M. Faraday, Philos. Trans. R. Soc. London **139**, 1 (1846).
 - [2] H. Perez Rojas and A. E. Shabad, Ann. Phys. **121** 432-455 (1979).
 - [3] H. Perez Rojas, J. Exp. Theor. Phys. **76**, 1 (1979).
 - [4] H. P. Rojas and E. R. Querts, International Journal of Modern Physics D **Vol. 19**, Nos. 810, 1599-1608 (2010).
 - [5] H. Perez Rojas and A. E. Shabad, Ann of Phys. **138** (1982) 1; H. Pérez Rojas, Informe Científico Técnico No. 71, junio de 1978.
 - [6] M. Giovannini, Phys. Rev. D **56**, 3198 (1997). 2186 1998.M.J. Rees, Q. J. R. Astron. Soc. 28, 197 (1987).P.P. Kronberg, Rep. Prog. Phys. 57, 325 1994.M. Giovannini, Phys. Rev. D **56**, 3198 (1997).A. Loeb and A. Kosowsky, Astrophys. J. **469**, 1 (1996).
 - [7] R. C. Duncan, arXiv:astro-ph/0002442.
 - [8] K. S. Novoselov, A. K. Geim, S. V. Morozov, D. Jiang, M. I. Katsnelson, I. V. Grigorieva, S. V. Dubonos, A. A. Firsov, Nature **438**, 197-200 (2005).
 - [9] A. H. Castro Neto, F. Guinea, N. M. R. Peres, K. S. Novoselov and A. K. Geim, Rev. Mod. Phys. **81**, 109-162 (2009).
 - [10] A. Perez Martinez, E. Rodriguez Querts, H. Perez Rojas, R. Gaitan, S. Rodriguez-Romo, J.Phys.A **44**, 445002, (2011), arXiv:1106.5722.
 - [11] Takahiro Morimoto, Yasuhiro Hatsugai, and Hideo Aoki, PRL **103**, 116803 (2009).
 - [12] J. C. Martínez, M. B. A. Jalil, S. G. Tan, J. Appl. Phys. **113**, 17B529 (2013).
 - [13] I Fialkovsky, DV Vassilevich Eur. Phys. J. B **85**, 384 (2012).
 - [14] Aires Ferreira, J. Viana-Gomes, Yu. V. Bludov, V. Pereira, N. M. R. Peres, and A. H. Castro Neto, Phys Rev B **84**, 235410 (2011).
 - [15] V.P. Gusynin and S.G. Sharapov, Phys. Rev. Lett. **95**, 146801 (2005).
 - [16] V. P. Gusynin, S. G. Sharapov, J. P. Carbotte, J. Phys Condens Matter **19**, 026222 (2007).
 - [17] V.P. Gusynin, S.G. Sharapov, J. P. Carbotte, New Journal of Physics **11**, 095013 (2009).
 - [18] Iris Crassee, Julien Levallois, Andrew L. Walter, Markus Ostler, Aaron Bostwick, Eli Rotenberg, Thomas Seyller, Dirk van der Marel, Alexey B. Kuzmenko Nature Physics **7**, 48 (2011).
 - [19] V A Volkov, S.A Mikhailov, Pisma Zh Eksp Teor.Fiz **41** No 9, 389-390 (1985).
 - [20] R. González Felipe and A. Pérez Martínez, Modern Physics Letters B, **Vol. 4**, No 17, 1103-1109 (1990).
 - [21] Avjit K. Ganguly, Sushan Konar and Palash B. Pal Phys Rev D Vol 60, 105014 (1999).
 - [22] Juan Carlos D'Olive, José F. Nieves and Sarira Sahu, Physical Review D **67**, 025018, (2003).
 - [23] E. S. Fradkin, Quantum Field Theory and Hydrodynamics. Proceeding of P.N. Lebedev, Consultant Bureau, New York (1967).
 - [24] Y. Ibeke, T. Morimoto, R. Masutomi, T. Okamoto, H. Aoki, R. Shimano, PRL **104**, 256802 (2010).
 - [25] V. Y. Zeitlin, Phys Lett **B**, **352**, 422 (1995).
 - [26] A. Khandler, R.F.OConnell and G. Wallace, Physical Review B **31**, 5208, (1985).
 - [27] J.D. Jackson, Classical Electrodynamics (John Wiley & Sons, New York, 1998).
 - [28] M. Born, E. Wolf, Principles of Optics: Electromagnetic Theory of Propagation, Interference and Diffraction of Light (Cambridge University Press, Cambridge, 1999).